Density Functional Theory Studies on Structure, Spectra, and Electronic Properties of 3,7-Dinitrodibenzobromolium Cation and Chloride

Xin Huai Zhang* and Yuan Ping Feng

Department of Physics, National University of Singapore, 2 Science Drive 3, Singapore 117542

Yu Zong Chen

Department of Computational Science, 3 Science Drive 2, Singapore 117543

Received: April 28, 2004; In Final Form: July 6, 2004

The structural and electronic properties of the 3,7-dinitrodibenzobromolium cation and chloride were studied using first-principle methods, based on the density functional theory (DFT). Different forms of exchange and correlation functions and basis sets were considered, and their suitability in studying such large molecules were assessed by comparing the calculated results with available X-ray diffraction data. The DFT results were also compared with those obtained previously using the Hartree−Fock (HF) method. The DFT methods improved on the calculated IR and Raman spectra, confirming the superiority of the DFT methods over the HF method in predicting harmonic frequencies, particularly for organic nitro compounds. The geometric parameters obtained using the hybrid DFT methods, such as B3LYP, B3P86, and B3PW91, are compatible with the results of the HF method. The structure of 3,7-dinitrodibenzobromolium chloride was optimized with and without symmetry constraints (such and C_s and C_{2v}) separately. The C_1 structure obtained from optimization without any symmetry constraints and the C_s structure were proven to be identical, using more-stringent convergence criteria in the structure optimization. Intrinsic reaction coordinate (IRC) calculation was performed, following the frequency calculation for the optimized C_{2v} structure. The results confirmed that the C_{2v} structure is the transition structure connecting the two energy minimum stuctures in C_s symmetry. A strong ionic bond is formed between the chloride anion and the 3,7-dinitrodibenzobromolium cation, with a Br−Cl bond length of 2.606 Å. Further studies were conducted to obtain the electronic density, electrostatic potential, and charge distribution of the chloride and the cation in its planar form and with the rotation of the nitro group. The charge distribution of other halides are also investigated and discussed. Knowledge of the electron properties is useful for understanding the bonding and biological activities of this molecule.

1. Introduction

Bromolium and iodolium heterocyclic compounds are a unique group of molecules that possess a wide range of biological activities. Extensive experimental studies have been performed recently to investigate the activities of these compounds.[1−3] However, because of the heavy atoms and complexity of the molecules, there have been very few theoretical or computational studies on such compounds. Theoretical investigation—particularly, computational studies, such as topology description, electronic structure, and molecular dynamics (MD) simulation—are useful in identifying and understanding the underlying mechanisms of the biological activities.

Previously, we performed an ab initio calculation based on the Hartree−Fock (HF) method on the 3,7-dinitrodibenzobromolium cation.[4] The HF method was observed to give an adequate description of the molecular structures, IR and Raman spectra, and electronic properties of the molecule. However, some predicted parameters, especially those belong to the nitro groups, have large deviations from experimental values that could be due to the neglect of electron correlation in the HF method. For the IR and Raman spectra, the frequencies pertaining to the symmetric and asymmetric vibrations of the nitro groups also have large deviations from the experimental frequencies.

Density functional theory (DFT) is an attractive alternative and complementary approach in the study of structural and electronic properties of molecules.[5−8] Because DFT accounts for electron correlation, and, on the other hand, it does not require more computational resources than the HF method or any other self-consistent field (SCF) approaches and it is much more efficient than the post-Hartree−Fock method, it is widely used in computational physics, chemistry, and material sciences, especially for systems that contain transition metals and systems in which electron correlation effect cannot be ignored.[9] Many previous works show that DFT methods give better results than the HF method in prediction of harmonic vibrational frequencies.[10−18] Jursic[19] used the DFT method to calculate the geometry and IR spectra of nitromethane, and he found that the DFT method outperformed the HF method. He recommended the use of B3LYP and B3PW91 in computational studies of the organic nitro compounds.

Thus, we further investigated the structure and electronic properties of the 3,7-dinitrodibenzobromolium cation using the DFT method. The structural and electronic properties of our DFT calculations are presented in the following sections and are compared with available experimental data, as well as with

* Author to whom correspondence should be addressed. E-mail: ccezxh@nus.edu.sg.

10.1021/jp048158j CCC: $27.50
Published on Web 08/20/2004

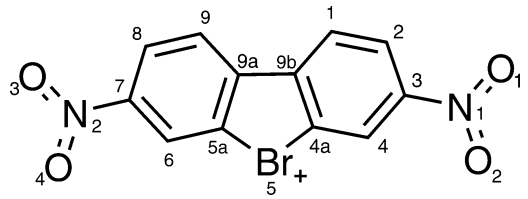

Figure 1. Structure of the 3,7-dinitrodibenzobromolium cation.

the HF results from previous calculations. Besides the cation form (Figure 1) considered in the earlier HF study, the present DFT calculation also considered the effects of the anion. The structure of the 3,7-dinitrodibenzobromolium chloride is optimized and its properties are investigated. Its structural parameters are also compared with those of the cation. The effects on the molecular structure and electronic properties due to rotation of the nitro group were further investigated, which is useful for understanding the bonding of the molecule and for further investigation on the biological activity of the molecule. The structures of other 3,7-dinitrodibenzohalolium chlorides were also optimized; the atomic charge distrubution in these molecules were compared and studied.

2. Computational Details

Structural optimization and calculation of harmonic vibrational frequencies were performed at the self-consistent field (SCF) level, based on the DFT study, using the Gaussian 98 software.[20] Various approximations for the exchange and correlation are available. To assess their suitability in the study of the bromolium heterocyclic compounds, the DFT calculations were performed using different forms of exchange and correlation. First, we used the local spin density approximation (LSDA) method[21−23] in combination with the Slater-Dirac exchange[24,25] and the Vosko, Wilk, and Nusair[26] correlation functional (SVWN). The gradient correlations then were introduced using the Becke exchange[27] and Lee, Yang, and Parr[28,29] correlation functionals. Finally, the combinations of the Becke's three-parameter hybrid exchange functional[30] with the gradient correlation functionals provided by Lee, Yang, and Parr[28,29] (B3LYP), Perdew−Wang's 1991 functional[31−33] (B3PW91), and Perdew's 1986 functional, along with his 1981 local correlation functional (B3P86),[34] respectively, were used in the calculation. Different basis sets were used with the B3LYP method to explore the basis set effect on the structure optimizations.

Structural optimizations with all the aforementioned methods were performed under the C_{2v} symmetry. The following convergence criteria (all given in atomic units) were imposed: maximum force, 0.00045, root-mean-square (rms) force, 0.0003, maximum displacement, 0.0018, and rms displacement, 0.0012. The optimization for the planar molecule with the C_{2v} symmetry converged for all the methods, and no imaginary frequencies were observed in the frequency analysis.

Structures of 3,7-dinitrodibenzobromolium chloride were optimized at the B3LYP/6-31G* level of theory, using the same convergence criteria. The molecules were optimized within the C_{2v} and C_s symmetry constraints and without symmetry constraints, respectively. With the symmetry constraints, the chloride ion is located along the axis of the molecule (C_{2v}) or in the plane of the molecule (C_s).

3. Structural Properties of the Cation

The optimizations of the cation using the B3LYP method with different basis sets all converged without any imaginary frequencies produced in the subsequent frequency calculation.

TABLE 1: Comparison of Bond Lengths Obtained Using the B3LYP Method with Different Basis Sets

	bond length (Å)				
	STO-3G	3-21G**	6-31G*	6-311+G*	expt
$r_{C_{5a}-C_{9a}}$	1.427	1.411	1.401	1.401	1.376
$r_{C_{9b}-C_{9a}}$	1.494	1.467	1.460	1.461	1.456
$r_{C_{4a}-C_{9b}}$	1.427	1.411	1.401	1.401	1.377
$r_{C_9-C_{9a}}$	1.424	1.407	1.404	1.404	1.395
$r_{C_6-C_{5a}}$	1.398	1.379	1.375	1.376	1.369
$r_{C_8-C_9}$	1.408	1.392	1.393	1.394	1.377
$r_{C_7-C_6}$	1.411	1.392	1.395	1.396	1.372
$r_{C_7-C_8}$	1.410	1.389	1.394	1.395	1.390
$r_{C_1-C_{9b}}$	1.424	1.407	1.404	1.404	1.389
$r_{C_1-C_2}$	1.408	1.392	1.393	1.394	1.392
$r_{C_4-C_{4a}}$	1.398	1.379	1.375	1.376	1.360
$r_{C_2-C_3}$	1.410	1.389	1.394	1.395	1.369
$r_{C_3-C_4}$	1.411	1.392	1.395	1.396	1.399
$r_{Br-C_{5a}}$	2.168	2.146	1.959	1.958	1.912
$r_{Br-C_{4a}}$	2.168	2.146	1.959	1.958	1.926
$r_{N_2-C_7}$	1.574	1.473	1.485	1.487	1.454
$r_{N_1-C_3}$	1.574	1.473	1.485	1.487	1.469
$r_{O_3-N_2}$	1.318	1.276	1.223	1.224	1.206
$r_{O_4-N_2}$	1.319	1.281	1.226	1.227	1.224
$r_{O_2-N_1}$	1.318	1.281	1.226	1.227	1.203
$r_{O_1-N_1}$	1.319	1.276	1.223	1.224	1.201
rms	0.101	0.078	0.021	0.021	

TABLE 2: Comparison of Bond Angles Obtained Using the B3LYP Method with Different Basis Sets

	bond angle (deg)				
	STO-3G	3-21G**	6-31G*	6-311+G*	expt
$A_{C_{5a}C_{9a}C_{9b}}$	118.1	118.2	116.2	116.1	115.3
$A_{C_{4a}C_{9b}C_{9a}}$	118.1	118.2	116.2	116.1	115.4
$A_{C_9C_{9a}C_{5a}}$	116.8	116.6	115.9	115.9	116.7
$A_{C_6C_{5a}C_{9a}}$	124.7	124.6	126.8	126.8	126.3
$A_{C_8C_9C_{9a}}$	120.5	120.5	120.3	120.4	120.3
$A_{C_7C_8C_9}$	119.4	119.7	119.7	119.7	118.9
$A_{C_6C_7C_8}$	122.9	122.5	122.9	122.9	123.6
$A_{C_1C_{9b}C_{4a}}$	116.8	116.6	116.1	115.9	117.3
$A_{C_4C_{4a}C_{9b}}$	124.7	124.6	126.8	126.8	126.7
$A_{BrC_{5a}C_{9a}}$	111.0	111.1	110.3	110.4	110.8
$A_{BrC_{4a}C_{9b}}$	111.0	111.1	110.3	110.4	111.1
$A_{C_{4a}C_5C_{5a}}$	81.8	81.4	87.0	87.0	86.7
$A_{C_7N_2O_3}$	116.0	116.2	116.6	116.8	119.9
$A_{C_7N_2O_4}$	116.0	116.2	116.5	116.7	118.2
$A_{O_3N_2O_4}$	128.0	127.6	126.8	126.5	122.7
$A_{C_3N_1O_2}$	116.0	116.2	116.5	116.7	118.8
$A_{C_3N_1O_1}$	116.0	116.2	116.6	116.8	118.5
$A_{O_1N_1O_2}$	128.0	127.6	126.8	126.5	122.7
rms	2.76	2.71	1.86	1.73	

As expected, the accuracy of the prediction increases as the basis sets increase; however, the increase corresponding to the increase of basis set from 6-31G* to 6-311+G* is only marginal (see Tables 1 and 2). This could be due to the fact that the structure of the cation is comparatively rigid and the 6-31G* basis set is large enough to give an accurate prediction; further increases in the basis set from 6-31G* do not offer much improvement. In this case, we will use 6-31G* for further investigations.

Bond lengths and bond angles of the cation molecule optimized using different ab initio methods were compared with those determined from X-ray diffractometry (XRD).[4] As shown in Tables 3 and 4, all methods produced bond lengths and bond angles that are in good agreement with experimental values. To assess the various methods, we computed the root-mean-square (rms) deviations of the calculated bond lengths and bond angles from the experimental data, and the results are also given in Tables 3 and 4. Table 3 shows that bond lengths given by SVWN, B3PW91, B3LYP, and B3P86 are comparable to those predicted using the HF method. However, the BLYP method

TABLE 3: Comparison of Bond Lengths Obtained Using Different Methods

	bond length (Å)						
	DFT						
	SVWN	BLYP	B3PW91	B3LYP	B3P86	HF	expt
$r_{C_{5a}-C_{9a}}$	1.397	1.411	1.399	1.401	1.398	1.388	1.376
$r_{C_{9b}-C_{9a}}$	1.442	1.466	1.456	1.460	1.454	1.469	1.456
$r_{C_{4a}-C_{9b}}$	1.397	1.412	1.399	1.401	1.398	1.388	1.377
$r_{C_9-C_{9a}}$	1.398	1.416	1.401	1.404	1.400	1.388	1.395
$r_{C_6-C_{5a}}$	1.369	1.382	1.374	1.375	1.373	1.368	1.369
$r_{C_8-C_9}$	1.385	1.402	1.390	1.393	1.389	1.386	1.377
$r_{C_7-C_6}$	1.388	1.407	1.393	1.395	1.391	1.384	1.372
$r_{C_7-C_8}$	1.387	1.404	1.392	1.394	1.390	1.383	1.390
$r_{C_1-C_{9b}}$	1.398	1.416	1.401	1.404	1.400	1.388	1.389
$r_{C_1-C_2}$	1.385	1.402	1.390	1.393	1.389	1.386	1.392
$r_{C_4-C_{4a}}$	1.369	1.382	1.374	1.375	1.373	1.368	1.360
$r_{C_2-C_3}$	1.387	1.404	1.392	1.394	1.390	1.383	1.369
$r_{C_3-C_4}$	1.388	1.407	1.393	1.395	1.391	1.384	1.399
$r_{Br-C_{5a}}$	1.921	1.995	1.937	1.959	1.936	1.930	1.912
$r_{Br-C_{4a}}$	1.921	1.995	1.937	1.959	1.936	1.930	1.926
$r_{N_2-C_7}$	1.468	1.507	1.480	1.485	1.477	1.463	1.454
$r_{N_1-C_3}$	1.468	1.507	1.480	1.485	1.477	1.463	1.469
$r_{O_3-N_2}$	1.220	1.242	1.217	1.223	1.217	1.187	1.206
$r_{O_4-N_2}$	1.223	1.244	1.220	1.226	1.220	1.191	1.224
$r_{O_2-N_1}$	1.220	1.242	1.217	1.223	1.217	1.187	1.203
$r_{O_1-N_1}$	1.223	1.244	1.220	1.226	1.220	1.191	1.201
rms	0.013	0.037	0.015	0.021	0.014	0.014	

TABLE 4: Comparison of Bond Angles Obtained by Different Methods

	bond angle (deg)						
	DFT						
	SVWN	BLYP	B3PW91	B3LYP	B3P86	HF	expt
$A_{C_{5a}C_{9a}C_{9b}}$	115.9	116.6	115.9	116.2	115.9	115.6	115.3
$A_{C_{4a}C_{9b}C_{9b}}$	115.9	116.6	115.9	116.2	115.9	115.6	115.4
$A_{C_9C_{9a}C_{5a}}$	116.4	115.4	116.0	115.9	116.1	116.6	116.7
$A_{C_6C_{5a}C_{9a}}$	126.5	127.3	126.7	126.8	126.7	126.2	126.3
$A_{C_8C_9C_{9a}}$	120.1	120.5	120.3	120.3	120.2	120.0	120.3
$A_{C_7C_8C_9}$	119.4	119.7	119.8	119.7	119.7	119.8	118.9
$A_{C_6C_7C_8}$	123.7	122.9	122.9	122.9	123.0	122.7	123.6
$A_{C_1C_{9b}C_{4a}}$	116.4	115.4	116.0	116.1	115.9	116.6	117.3
$A_{C_4C_{4a}C_{9b}}$	125.5	127.3	126.7	126.8	126.7	126.2	126.7
$A_{BrC_{5a}C_{9a}}$	110.2	110.1	110.4	110.3	110.3	110.7	110.8
$A_{BrC_{4a}C_{9b}}$	110.2	110.1	110.4	110.3	110.3	110.7	111.1
$A_{C_{4a}BrC_{5a}}$	87.8	86.4	87.5	87.0	87.4	87.4	86.7
$A_{C_7N_2O_3}$	116.4	119.6	116.6	116.6	116.6	116.9	119.9
$A_{C_7N_2O_4}$	116.3	119.4	116.5	116.5	116.6	116.6	118.2
$A_{O_3N_2O_4}$	127.3	126.9	126.9	126.8	126.9	126.5	122.7
$A_{C_3N_1O_2}$	116.4	119.6	116.6	116.6	116.6	116.9	118.8
$A_{C_3N_1O_1}$	116.3	116.4	116.5	116.5	116.6	116.6	118.5
$A_{O_1N_1O_2}$	127.3	126.9	126.9	126.8	126.0	126.5	122.7
rms	2.03	1.74	1.87	1.86	1.76	1.67	

yields slightly larger deviations in the bond lengths. On the other hand, qualities of bond angles obtained using BLYP, B3PW91, B3LYP, and B3P86 are comparable to those of the HF calculation, but the SVWN method gives a large deviation from experimental values. Generally, as far as the molecular structure is concerned, the levels of accuracy of the DFT methods are the same as the HF method and the DFT calculations do not give any significant improvement for the geometric structure of the 3,7-dinitrodibenzobromolium cation over the HF method. Therefore, we conclude that the HF and DFT calculations both can accurately predict the geometry of such molecules.

In each of the DFT results, as in the HF result, the poorest prediction comes from the bond lengths and bond angles of the nitro groups. The calculated bond angles related to the nitro group, particularly the O−N−O bond angle, have larger deviations from the corresponding experimental values. Compared to the HF method, which predicted O−N bonds shorter than the experimental values, the DFT yields slightly longer O−N bonds than the experimental values. The O−N−O bond angle given by the HF method is much larger than the experimental value. The DFT calculations give similar values and have little improvement over the HF results. Based on his studies on the structure and IR spectra of nitromethane using the DFT method, Jursic[19] concluded that the B3LYP method outperforms the ab initio (HF, MP2, MCSCF) methods and the SVWN and BLYP methods. Results of the present study suggest that, as far as structural parameter prediction is concerned, the B3LYP, B3PW91, and B3P86 are comparable and give the same level of accuracy as the HF method, while the qualities of the calculated bond lengths and bond angles by SVWN and BLYP are inconsistent. All methods give poor predictions of the structural parameters of the nitro group.

Harmonic vibrational frequencies were calculated using various methods, and all DFT methods gave better predictions for the vibrational frequencies than the HF method. Among them, results obtained using the B3LYP method with the 6-31G* basis set have the smallest deviation from the measured values and are shown in Table 5. The frequencies were scaled by a factor of 0.9614, which was suggested by Scotta and Radom[39] for the B3LYP/6-31G* method to eliminate the known systematic errors. With the HF method, the deviation between the calculated and experimental results for the symmetrical and asymmetrical stretch in the nitro groups are as large as 139 and 178 cm^{-1}, and those by the B3LYP method are 11 and 93 cm^{-1}, respectively. This demonstrates that the DFT methods—especially, the B3LYP method—give better IR and Raman frequencies for the organic nitro compounds, even though it still overestimates the experimental value in the high-frequency regions.

4. Rotation of the Nitro Groups

In the HF studies, we concluded that there is no conjugation between the nitro group and the benzoid plane by observing the changes in the geometric parameter, relative to the rotation of the nitro group. To further investigate the potential energy and the electron density change with the rotation of the nitro group, we performed structural optimization while fixing the dihedral angle at various values. This was done by fixing the atoms in the nitro group in one plane and rotating the nitro group along the C−N bond to change the dihedral angle between the planar nitro group and the benzoid plane. Structural optimization was performed for each structure with a certain dihedral angle, using the B3LYP method with the 6-31G* basis set, which was followed by frequency analysis to determine the structural stability by examining whether the given configuration is a stationary point or a saddle point in the potential energy surface. Because the electron density is a basic physical property and it is closely related to the structure and configuration of the molecules, by observing the electron density change with the rotation of the nitro group, we will be able to further confirm the conjugation of the nitro group and clarify the electronic structure of the molecule.

The response of charge density near each of the concerned atoms to the rotation of the nitro group is shown in Figure 2, whereas the corresponding potential energy is shown in Figure 3. According to the magnitudes of change and trends shown in Figures 2 and 3, we can see three different types of responses to the rotation of the nitro group. When the dihedral angle is small (<10°), changes in the electron density on each atom and in total energy are very small. The small rotation of the nitro group does not produce any significant changes to the molecular

TABLE 5: Comparison of Theoretical and Experimental IR and Raman Frequencies[a]

		IR				Raman					
		theory		expt		theory		expt			
no.[b]	symmetry	freq (cm^{-1})	int[c]	freq (cm^{-1})	int[d]	freq (cm^{-1})	int[e]	freq (cm^{-1})	int[e]	depol[f]	mode description[g]
24	B_2	629	26.7	592	s	629	3.6	*h*		0.75	CH ip bend
25	B_1	662	0.0	641	w	662	0.6			0.75	CH bend, ring defm
26	A_1	662	10.7	686	m	662	15.7	690	m	0.09	CH opp bend
27	B_2	665	50.7	700	s	665	0.2			0.75	NO_2 defm
28	A_2	691	0.0			691	0.2			0.75	CH oop bend
29	B_1	713	51.3	736	s	713	0.2			0.75	CH, CN oop bend
30	A_2	728	0.0			728	8.6	753	m	0.75	CH, NO oop bend
31	A_1	744	0.4			744	1.8			0.13	NO_2 scissor
32	B_2	821	95.6	828	s	821	0.0			0.75	NO_2 scissor
33	B_1	829	33.2	856	s	829	3.9			0.75	CH oop bend
34	A_2	847	0.0			847	0.1			0.75	CH oop bend
35	A_1	847	8.4	886	m	847	22.9	878	m	0.11	NO_2 defm
36	A_2	895	0.0			895	3.9			0.75	CH oop bend
37	B_1	896	33.7	915	m	896	0.8			0.75	CH oop bend
38	B_2	955	38.1	985	m	955	1.6			0.75	ring defm, CH bend
39	A_2	969	0.0		m	969	3.7			0.75	CH oop bend
40	B_1	971	1.8			971	0.0			0.75	CH oop bend
41	A_1	986	11.2	1022	m	986	4.1	1017	w	0.12	CH ip bend
42	B_2	1032	2.0			1032	0.0			0.75	CH ip bend
43	B_2	1068	161.5	1078	s	1068	0.8			0.75	CC str, CH bend
44	A_1	1075	2.6			1075	124.3	1115	m	0.25	CH ip bend
45	A_1	1112	4.3	1107	s	1112	62.3	1130	m	0.24	CH ip bend
46	B_2	1118	5.6	1130	m	1118	0.0			0.75	CH ip bend
47	A_1	1207	0.9			1207	30.4			0.32	CH ip bend
48	B_2	1231	1.3	1229	s	1231	0.7			0.75	CH ip bend
49	A_1	1282	0.0			1282	313.4	1300	s	0.29	CH ip bend
50	B_2	1307	20.0	1281	m	1307	9.9			0.75	ring defm
51	A_1	1312	0.1			1312	213.5	1326	m	0.25	CH ip bend
52	A_1	1330	659.5	1341	vs	1330	3.4			0.75	NO_2 sym str
53	B_2	1334	4.9	1342	m	1334	374.1	1349	vs	0.25	NO_2 sym str
54	B_2	1362	52.5	1375	m	1362	15.7			0.20	CH bend, CC str
55	A_1	1391	12.7	1398	w	1391	10.0			0.75	CH ip bend
56	B_2	1434	49.1	1449	w	1434	0.2			0.75	CH ip bend
57	A_1	1464	0.0			1464	72.6			0.27	ring tor
58	B_2	1543	7.5			1543	1.8			0.75	ring str
59	A_1	1545	51.1	1537	s	1545	195.7			0.31	ring tor
60	A_1	1582	12.0	1591	m	1582	1918.9	1593	vs	0.36	ring str, CH wag
61	B_2	1586	0.0	1591	m	1586	0.1			0.75	ring str, CH wag
62	A_1	1618	296.2	1525	vs	1618	4.1			0.39	NO_2 asym str
63	B_2	1619	3.2	1525	vs	1619	28.7			0.75	NO_2 asym str
64	B_2	3100	0.1	3026	s	3100	8.5			0.75	CH str
65	A_1	3105	0.2	3027	s	3105	82.6			0.34	CH str
66	B_2	3127	25.8	3045	s	3127	32.9			0.75	CH str
67	A_1	3127	36.9	3046	s	3127	91.0			0.10	CH str
68	B_2	3130	18.5	3078	s	3130	55.5			0.75	CH str
69	A_1	3130	13.6	3079	s	3130	159.3			0.11	CH str

[a] The theoretical values were obtained using the B3LYP method with the 6-31G* basis set. [b] Number in the order, from the calculated results. [c] IR intensity, based on units of kM/mol. [d] Relative intensity: vs, very strong; s, strong; m, medium; w, weak. [e] Raman intensity, based on units of A^4/amu. [f] Depolarization ratio. [g] Abbreviations for mode description are as follows: str, stretch; bend, bending; scissor, scissoring; wag, wagging; tor, torsion; defm, deformation; ip, in-plane; and oop, out-of-plane. [h] Frequency not observed, because of the low intensity and limited resolution.

structure and properties. When the dihedral angle is further increased, up to ~60°, there are significant changes (mostly decreases) in the electron density on the concerned atoms and the total energy of the molecule increases rapidly. All vibrational frequencies of the optimized geometries are real. The structure is stable. However, when the nitro group is rotated by >60°, dramatic changes (mostly increases) in the electron density on the concerned atoms are observed, and the energy of the molecule increases slowly. Frequency analysis reveals that two of its frequencies are imaginary, which suggests a second-order saddle point in the potential energy surface.

If there is, indeed, a conjugation between the nitro group and the benzoid plane, the rotation of the nitro group will cause the conjugation to break, and a certain amount of energy would be required for this to occur. Figure 3 shows that the average rate of energy increase is only 0.027 kcal mol^{-1} deg^{-1} in the first stage and the density changes on the concerned atoms are very small. The electron density near these atoms is the highest when the molecule is planar. Referring back to the HF study, we confirm that there is no conjugation between the nitro group and the benzoid plane. In the second stage, as the dihedral angle increases, the change in the configuration of the molecule becomes large enough to influence the molecular orbitals and both the shape and the sequence of orbitals change. This has been observed in the molecular orbital calculation. Thus, the electron distribution has also changed. In the third stage, the nitro group is almost perpendicular to the benzoid plane. There could be some interactions between the molecular orbital on nitro groups and the benzoid ring, and it could be this interaction that causes the dramatic change of the electron density on the O atoms.

Naturally, the nitro group may not be able to rotate too much along the C−N bond. However, the fact that the frequency calculations for the optimized structures with a dihedral angle

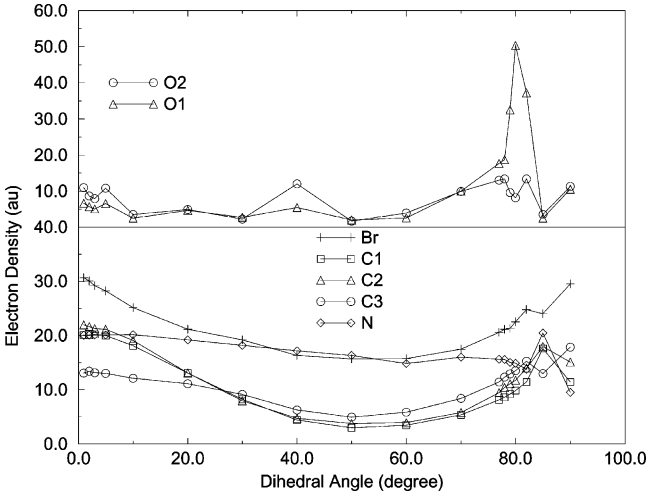

Figure 2. Response of the electron density near the concerned atoms with the rotation of the nitro group.

of <60° gave no imaginary frequencies suggests that the nitro groups can rotate, to a certain degree, under external forces. For example, it was observed in the X-ray crystal structure that the two O atoms of the nitro group are actually out of the plane of the molecule.[3]

5. Optimization of the Chloride

The optimization of the chloride with and without symmetry constraints all converged. The total energies of the optimized structures, as well as the structural parameters, the angle Cl−Br−C_6, and the dihedral angle Cl−Br−C_6−C_7, are listed in Table 6. The frequency calculations that follow the optimization with the C_s symmetry constraint and the optimization without any symmetry constraints (C_1) give no imaginary frequencies, which means that the structures that are optimized in these cases are energy minima. The energy difference, as well as the differences between the corresponding bond lengths and bond angles in these two cases are quite small, and the differences become even smaller as more-stringent convergence criteria are used. Therefore, we can conclude that these two structures are identical. The frequency calculation following the optimization with the C_{2v} point group gives one imaginary frequency, indicating that the C_{2v} structure is a transition structure. The intrinsic reaction coordinate (IRC)[40−42] calculation on the B3LPY/6-31G* level of theory was conducted, to further investigate the transition structure. The IRC calculation confirms that the C_{2v} structure is the transition structure that connects two energy minima in C_s symmetry. In one of the energy minimum structures, the chloride ion resides on the left side of the molecule and in the other structure, it resides on the right side. The energy of the two C_s structures in the IRC calculation is quite similar to that of the C_s structure that we obtained during the direct geometry optimization. The energy difference between the transition structure and the energy minima−16.75 kcal/mol (0.0267 Hartree)—is the energy barrier preventing the chloride ion from moving from one side of the molecule to the other side, through the C_{2v} transition structure.

The Br−Cl bond lengths in the optimized C_s and C_1 structures are ∼2.606 Å (see Table 6), which is larger than the sum of the covalent radii of bromine and chlorine (2.132 Å) and smaller than the sum of their van der Waals radii (3.76 Å); we conclude that the bond between the 3,7-dinitrodibenzobromolium cation and the chloride ion is mainly ionic in nature. Therefore, the chloride ion does not have much influence on the bond lengths and bond angles of the cation.

TABLE 6: Optimized Structure Parameters for Chloride with Different Symmetry Constraints

symmetry group	total energy (hartree)	C_{5a}−Br−Cl (deg)	C6−C_{5a}−Br−Cl (deg)	Br−Cl (Å)
C_1	−3902.92445478	93.78	0.038	2.606
C_s	−3902.92444133	93.81	0.0	2.605
C_{2v}	−3902.89974482	138.65	0.0	2.661

6. Electronic Properties

The calculated electrostatic potential (EP) for the 3,7-dinitrodibenzobromolium chloride is shown in Figure 4, using a two-dimensional contour plot. The EP explicitly reflects the net effect of all nuclei and electrons at each point in space. The sign of the EP in any particular region is dependent on whether the effects of the nuclei or the electrons are dominant and is directly related to its activity at the given region. Regions in which the EP is negative will exert attractions to the electrophiles. In the case of 3,7-dinitrodibenzobromolium chloride, the negative regions are found near the O and Cl atoms. These regions would have greater affinity to positive sites of a target molecule.

Regions with a negative EP cannot be found in the central part, on either side of the planar molecule. This coincides with the findings by Murray et al.[43] who concluded that strongly electron-withdrawing substitutes (such as −CN, $-NO_2$, −CHO) either totally eliminate negative regions above and below the aromatic ring or significantly weaken them.

To allow the EP to be used to interpret nucleophilic processes, Politzer and co-workers[44−49] developed techniques to present the EP using a two- or three-dimensional surface significantly remote from the nuclei. Such a surface reveals the buildups of positive potential that reflects relative affinities for nucleophiles. It was found that this surface electron potential is useful for understanding the noncovalent interactions, such as hydrogen bonding and biological recognition. The EP is computed on the molecular surface defined in terms of the electronic charge density and the surface is taken to correspond to the 0.002 e/bohr^3 isosurface of electron density in this study. We calculated the EP on this isoelectron density surface for the 3,7-dinitrodibenzobromolium cation. The EP values on this surface are in the range of 24.4−225 kcal/mol, with the minimum near the O atoms and the maximum value near the Br atom, and no negative regions are found. These features reflect the electron-attracting ability of the cation. Therefore, we can expect that the bromolium heterocyclic compounds can easily combine with a DNA molecule as an intercalator or groove binding agent, as the groove regions of the DNA molecules are generally electron negative, because of the sugar phosphates in the backbone. Actually, it has been found that planar cationic molecules can bind to DNA molecules as intercalators or groove binding agents, which cause the cessation of normal cellular functions regulated by DNA. Some of them have been developed into anti-cancer drugs.[50−53] Our calculation provides further physical insight to the binding mechanism, from the point of view of electronic structure of the molecule.

The charge distribution of a molecular system is of great importance to its structure and activity. Theoretically determined atomic charges are also useful in MD simulation. The charges derived from least-squares fitting to the EP are widely used for this purpose. Various schemes, which mainly differ in the choice of the points where the EP is calculated, and the different algorithms used are proposed for deriving charges from potentials. Among these, the Merz−Kollman[36] and the ChelpG[37] schemes are the most widely used. In the present study, atomic

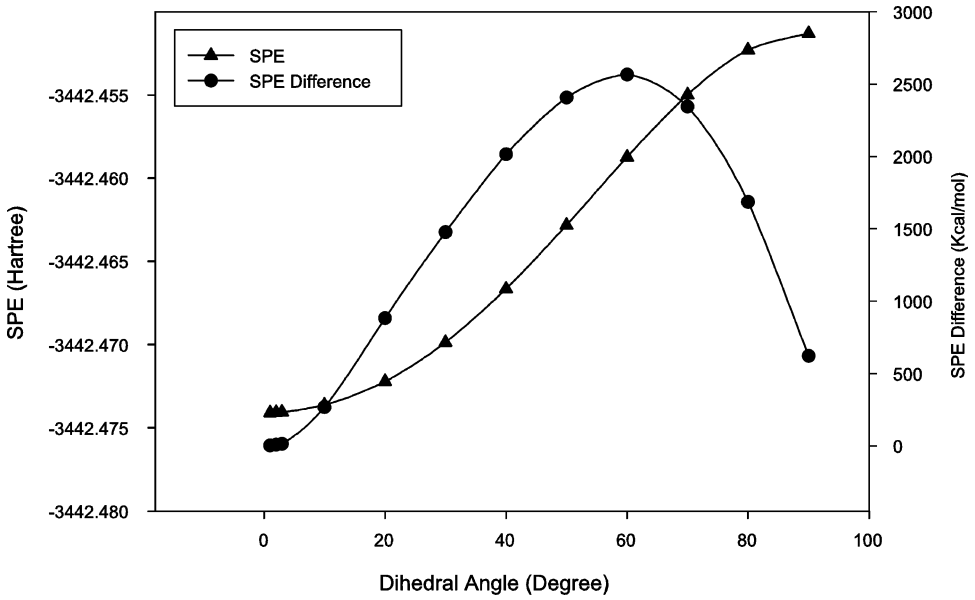

Figure 3. Potential energy of the molecule, relative to the rotation of the nitro group.

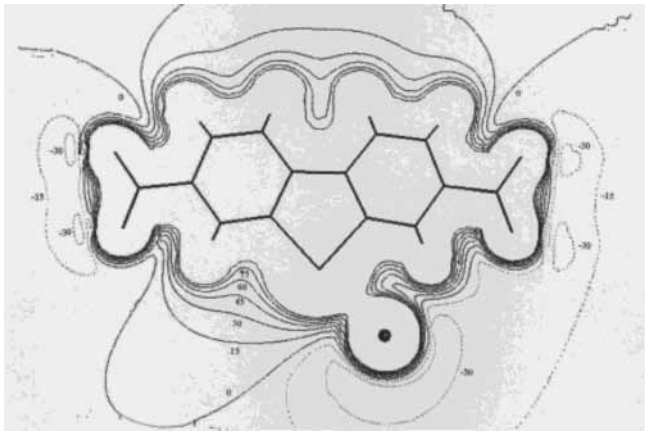

Figure 4. Electrostatic potential of the 3,7-dinitrodibenzobromolium chloride.

charges were calculated for the cation and chloride using the Merz−Kollman scheme and the ChelpG scheme, respectively. The results are given in Table 7. A van der Waals radius of 168 nm, obtained from ref 38, is used for the Br atom in the ChelpG scheme.

In regard to the atomic charges for the cation and the chloride molecule, we notice that, compared to the ChelpG method, the MK method produces relatively larger charge differences on atoms C_4, C_{4a}, and Br, which are near the Cl atom in the molecule. The charges of the cation and the chloride by ChelpG are more consistent. The large variation in the MK charges may be due to the implementation of the scheme in the Gaussian code. According to Fox,[54] the algorithms used by the MK scheme include a step where surface points are generated, relative to the principal axis created at each atom and then a unit sphere rolls around the molecule. If the principal axis for this surface generation goes from in plane to perpendicular or vice versa, some variation may occur. This problem does not happen in the ChelpG scheme, because the ChelpG algorithm uses different ways to sample the space. In the case of bromolium heterocyclic compounds, we can see that ChelpG gives a better description of the atomic charge.

Based on the aforementioned observation, we also conducted ChelpG charge calculations on the other haloliums of the same serial, the 3,7-dinitrodibenzohalolium chlorides. For a better comparison, all the 3,7-dinitrodibenzohalolium chlorides are optimized using the B3LYP method and the 3-21G** basis set before the ChelpG charges are calculated. The results are listed in Table 8. A few observations were obtained from this table: (a) charges on the halolium atoms become more positive, from the fluorolium to the iodolium chloride; (b) from the fluorolium to the iodolium chloride, charges on N and O atoms change very little, except that on O_2, which has a change of 0.037 or 10.7% increase. (c) Dramatic changes are observed for charges on those C atoms that are very near to halolium atoms, such as C_{4a} and C_{5a}. Apart from all these changes, it can be seen that atomic charges on the fluorolium are nearer to the corresponding charges on the chlorolium, whereas the atomic charges on the bromolium are nearer to the corresponding charges on the iodolium.

TABLE 7: Atomic Charges of the 3,7-Dinitrodibenzobromolium Cation and Chloride

	cation		chloride	
atom	MK	ChelpG	MK	ChelpG
C_1	−0.106	−0.105	−0.217	−0.116
C_2	−0.095	−0.022	−0.129	−0.071
C_3	0.082	0.045	0.035	0.006
C_4	−0.136	−0.108	0.047	0.009
C_{4a}	−0.085	-0.051	−0.209	−0.023
C_{5a}	−0.085	−0.051	0.198	−0.047
C_6	−0.136	−0.108	−0.316	−0.122
C_7	0.082	0.045	0.077	0.009
C_8	−0.095	−0.022	−0.173	−0.054
C_9	−0.106	−0.105	−0.060	−0.132
C_{9a}	0.087	0.090	−0.153	0.076
C_{9b}	0.087	0.090	0.278	0.051
Br	0.495	0.450	0.306	0.354
N_1	0.611	0.600	0.616	0.606
N_2	0.611	0.600	0.674	0.625
O_1	−0.321	−0.314	−0.377	−0.375
O_2	−0.337	−0.346	−0.341	−0.375
O_3	−0.321	−0.314	−0.384	−0.367
O_4	−0.337	−0.346	−0.382	−0.381
H_1	0.166	0.150	0.166	0.121
H_2	0.174	0.141	0.170	0.132
H_3	0.213	0.197	0.125	0.115
H_4	0.213	0.197	0.134	0.128
H_5	0.174	0.141	0.169	0.119
H_6	0.166	0.150	0.222	0.175
Cl			−0.479	−0.507

TABLE 8: ChelpG Charges of the 3,7-Dinitrodibenzohalolium Chlorides

	charge			
atom	fluorolium	chlorolium	bromolium	iodolium
C_1	−0.113	−0.155	−0.172	−0.176
C_2	−0.176	−0.120	−0.097	−0.098
C_3	0.034	−0.029	−0.045	−0.043
C_4	−0.181	−0.047	−0.025	−0.050
C_{4a}	0.250	−0.012	−0.079	−0.084
C_{5a}	0.174	0.017	−0.084	−0.120
C_6	−0.215	−0.171	−0.133	−0.144
C_7	0.024	−0.034	−0.055	−0.055
C_8	−0.154	−0.100	−0.087	−0.075
C_9	−0.112	−0.135	−0.147	−0.169
C_{9a}	0.005	0.013	0.044	0.068
C_{9b}	−0.045	0.063	0.084	0.068
halide	0.030	0.310	0.416	0.461
Cl	−0.532	−0.525	−0.479	−0.401
N_1	0.634	0.658	0.662	0.662
N_2	0.633	0.643	0.635	0.643
O_1	−0.350	−0.358	−0.361	−0.365
O_2	−0.345	−0.368	−0.374	−0.382
O_3	−0.365	−0.367	−0.364	−0.369
O_4	−0.329	−0.335	−0.338	−0.349

Note that there are positive charge centers around the halolium atoms and the N atoms, whereas the O atoms carry negative charges. Looking back at Figure 4, which depicts the EP of 3,7-dinitrodibenzobromolium chloride, the negative potential areas are observed near O atoms, and it can be suggested that both ends of the 3,7-dinitrodibenzobromolium cation can be easily attached to high-potential regions of molecules, such as in the grave of a DNA double helix, whereas its central parts are attractive to negative ions or molecules.

7. Conclusion

Structural and electronic properties of the 3,7-dinitrodibenzobromolium cation were investigated using first-principle methods, based on the density functional theory (DFT), with various forms of exchange and correlation functional and different basis sets. Structural parameters such as bond lengths and bond angles given by the DFT methods are of the same level of accuracy as the HF method, when compared with the XRD data. Better agreement between the calculated harmonic frequencies and the experiment results are obtained with the hybrid DFT methods. The structure parameters in the optimized 3,7-dinitrodibenzobromolium chloride and the cation are almost the same. An ionic bond is formed between the chloride ion and the 3,7-dinitrodibenzobromolium cation. The C_{2v} structure of 3,7-dinitrodibenzobromolium chloride is proved to be the transition structure connecting the two energy minimum stuctures in C_s symmetry. The investigation of the potential energy and the electron density changes with the rotation of the nitro group indicate that there is no conjugation between the nitro group and the benzoid plane. Electron density distribution and electrostatic potential of the compound were calculated, and these studies show that, because of the electron positivity of the molecular surface, intercalation or groove-binding to the DNA strands is suitable for this type of molecule.

References and Notes

(1) Chen, S.; Wang, C.; Li, D.; Wang, X. *Sci. China Ser. B* **1986**, *32*, 918.
(2) Liu, L.; Zheng, R.; Hou, Z. *Kexue Tongbao* **1989**, *10*, 783.
(3) Hou, Z.; Zhu, Y.; Wang, Q. *Sci. China Ser. B* **1996**, *39*, 262.
(4) Zhang, X. H.; Feng, Y. P.; Hou, Z. J. *J. Phys. Chem. A* **1998**, *102*, 9261.
(5) Parr, R. G.; Yang, W. *Density-Functional Theory of Atoms and Molecules*; Oxford University Press: New York, 1989.
(6) Labanowski, J. K.; Andzelm, J. W. *Density Functional Method in Chemistry*; Springer−Verlag: New York, 1991.
(7) Ziegler, T. *Chem. Rev.* **1990**, *91*, 651.
(8) Kohn, W.; Becke, A. D.; Parr, R. G. *J. Phys. Chem.* **1996**, *100*, 12974.
(9) Stephens, P. J.; Delvin, F. J.; Chabalowski, C. F.; Frisch, M. J. *J. Phys. Chem.* **1994**, *99*, 11623.
(10) Delvin, F. J.; Finley, J. W.; Stephens, P. J.; Frisch, M. J. *J. Phys. Chem.* **1995**, *99*, 16883.
(11) El-Azhary, A. A.; Suter, H. U. *J. Phys. Chem.* **1995**, *99*, 12751.
(12) Wheeless, C. F. M.; Zhou, X.; Liu, R. *J. Phys. Chem.* **1995**, *99*, 12488.
(13) Rauhut, G.; Pulay, P. J. *J. Phys. Chem.* **1995**, *99*, 3039.
(14) Jonhson, B. G.; Gill, P. M. W.; Pople, J. A. *J. Chem. Phys.* **1993**, *98*, 5612.
(15) Langhoff, S. R. *J. Phys. Chem.* **1996**, *100*, 2819.
(16) Miaskiewicz, K.; Smith, D. A. *Chem. Phys. Lett.* **1997**, *270*, 376.
(17) Lee, S. Y.; Boo, B. H. *J. Phys. Chem.* **1996**, *100*, 15073.
(18) El-Azhary, A. A.; Suter, H. U.; Kubelka, J. *J. Phys. Chem. A* **1998**, *102*, 620.
(19) Jursic, B. S. *Int. J. Quantum Chem.* **1997**, *64*, 263.
(20) Frisch, M. J.; Trucks, G. W.; Schlegel, H. B.; Scuseria, G. E.; Robb, M. A.; Cheeseman, J. R.; Zakrzewski, V. G.; Montgomery, J. A., Jr.; Stratmann, R. E.; Burant, J. C.; Dapprich, S.; Millam, J. M.; Daniels, A. D.; Kudin, K. N.; Strain, M. C.; Farkas, O.; Tomasi, J.; Barone, V.; Cossi, M.; Cammi, R.; Mennucci, B.; Pomelli, C.; Adamo, C.; Clifford, S.; Ochterski, J.; Petersson, G. A.; Ayala, P. Y.; Cui, Q.; Morokuma, K.; Malick, D. K.; Rabuck, A. D.; Raghavachari, K.; Foresman, J. B.; Cioslowski, J.; Ortiz, J. V.; Stefanov, B. B.; Liu, G.; Liashenko, A.; Piskorz, P.; Komaromi, I.; Gomperts, R.; Martin, R. L.; Fox, D. J.; Keith, T.; Al-Laham, M. A.; Peng, C. Y.; Nanayakkara, A.; Gonzalez, C.; Challacombe, M.; Gill, P. M. W.; Johnson, B. G.; Chen, W.; Wong, M. W.; Andres, J. L.; Head-Gordon, M.; Replogle, E. S.; Pople, J. A. *Gaussian 98*, revision A.6; Gaussian, Inc.: Pittsburgh, PA, 1998.
(21) Hohenberg, P.; Kohn, W *Phys. Rev. B* **1964**, *136*, 864.
(22) Kohn, W.; Sham, L. J. *Phys. Rev. A* **1965**, *140*, 1133.
(23) Slater, J. C. *The Self-Consistent Field for Molecular and Solids*; Quantum Theory of Molecular and Solids, Vol. 4; McGraw-Hill: New York, 1974.
(24) Dirac, P. A. M. *Proc. Cambridge Philos. Soc.* **1930**, *26*, 376.
(25) Slater, J. C. *Phys. Rev.* **1951**, *81*, 385.
(26) Vosko, S. J.; Wilk, L.; Nusair, M. *Can. J. Phys.* **1980**, *58*, 1200.
(27) Becke, A. D. *Phys. Rev.* **1988**, *A38*, 3098.
(28) Lee, C.; Yang, W.; Parr, R. G. *Phys. Rev.* **1988**, *B37*, 785.
(29) Miehlich, B.; Savin, A.; Stoll, H.; Preuss, H. *Chem. Phys. Lett.* **1989**, *157*, 200.
(30) Becke, A. D. *J. Chem. Phys.* **1993**, *98*, 5648.
(31) Perdew, J. P. *In Electronic Structure of Solids '91*; Ziesche, P., Eschrig, H., Eds.; Akademie Verlag: Berlin, 1991.
(32) Perdew, J. P.; Wang, Y. *Phys. Rev.* **1986**, *B33*, 8800.
(33) Perdew, J. P.; Burke, K.; Wang, Y. *Phys. Rev.* **1996**, *B54*, 16533.
(34) Perdew, J. P. *Phys. Rev.* **1986**, *B33*, 8822.
(35) *Unichem 5.0* Oxford Molecular, Oxford, U.K., 2000.
(36) Besler, B. H.; Merz, K. M., Jr.; Kollman, P. A. *J. Comput. Chem.* **1990**, *11*, 431.
(37) Breneman, C. M.; Wiberg, K. B. *J. Comput. Chem.* **1990**, *11*, 361.
(38) Bondi, A. *J. Phys. Chem.* **1964**, *68*, 441.
(39) Scott, A. P.; Radom, L. *J. Phys. Chem.* **1996**, *100*, 16502.
(40) Foresman, J. B.; Frisch, A. *Exploring Chemistry with Electronic Structure Methods*; Gaussian, Inc.: Pittsburgh, PA, 1996.
(41) Fukui, K. *Acc. Chem. Res.* **1981**, *14*, 163.
(42) Gonzalez, C.; Schlegel, H. B. *J. Phys. Chem.* **1990**, *94*, 5523.
(43) Murray, J. S.; Paulsen, K.; Politzer, P. *Proc. Ind. Acad. Sci. (Chem. Sci.)* **1994**, *106*, 267.
(44) Politzer, P.; Abrahamsen, L.; Sjoberg, P. *J. Am. Chem. Soc.* **1984**, *106*, 855.
(45) Politzer, P.; Laurance, P. R.; Abrahamsen, L.; Zilles, B. A.; Sjoberg, P. *Chem. Phys. Lett.* **1984**, *111*, 75.
(46) Murray, J. S.; Lane, P.; Politzer, P. *J. Mol. Strut. (THEOCHEM)* **1990**, *209*, 163.
(47) Murray, J. S.; Sjoberg, P.; Politzer, P. *J. Phys. Chem.* **1990**, *94*, 3959.
(48) Murray, J. S.; Lane, P.; Brinck, T.; Politzer, P.; Sjoberg, P. *J. Phys. Chem.* **1991**, *95*, 844.
(49) Politzer, P.; Laudry, J.; Warnheim, T. *J. Phys. Chem.* **1982**, *84*, 4767.
(50) Lerman, L. S *J. Mol. Biol.* **1961**, *1*, 18.
(51) Wilson, D.; Jones, R. *Intercalation Chemistry*; Academic Press: New York, 1982; pp 445−501.
(52) Monaco, R. R.; Polkosnik, W. *J. Biomol. Struct. Dyn.* **1996**, *14*, 13.
(53) Monaco, R. R.; Polkosnik, W.; Dwarakanath, S. *J. Biomol. Struct. Dyn.* **1997**, *15*, 63.
(54) Fox, D. J., Gaussian, Inc., personal communication, 2002.